ATMOSPHERIC CORRECTION OF LANDSAT/TM DATA OVER MOUNTAINOUS TERRAIN

G. Kattenborn
Albert-Ludwigs-Universität
Abteilung Luftbildmessung und Fernerkundung
Werderring 6, 7800 Freiburg, Germany
ISPRS Commission VII

ABSTRACT:

A method to correct atmospheric effects on Landsat/TM data over mountainous terrain in the solar spectrum was developed primarily for forestry applications, but can also be adapted to other sensors and applications. The algorithm automatically identifies patches of dense, dark vegetation as controllable dark surfaces for the purpose of estimating aerosol optical thickness. Thereby a network of radiometric control points, rendering both horizontal as well as relief induced vertical changes of atmospheric conditions, is expanded over a scene. Atmospheric parameters calculated with LOWTRAN over these pixels are smoothed and interpolated by cubic spline regression. With these values atmospherically corrected ground reflectances are calculated pixelwise by iteration of a correction model. Improvements in visual interpretation, in the standardization of photo products and in the use of calibrated data with multitemporal applications are discussed.

KEY WORDS: Atmospheric Correction, Landsat, Multitemporal Applications, Standardized Photo Products

1. INTRODUCTION

A number of remote sensing satellites such as the Landsat series have produced encouraging results for the application over land and water bodies. The importance of monitoring tasks and of input into information systems grow steadily as opposed to single evaluations. This developement leads to the demand for a standardization method for the ever increasing amount of heterogenous multitemporal, multisensor and multiangle data.

The distortion of surface signals by external conditions during the sensing aggravate the qualitative and quantitative data interpretation and the comparison of different data sets in both visual and digital interpretation. Particularly forestry evaluations of multispectral data which are frequently taken over mountainous terrain suffer from vertical (Hildebrandt et al., 1987; Kattenborn, 1987) and horizontal (Schardt, 1991) atmosphere inhomogenities. It is therefore desirable to standardize data sets taken at different dates or places by eliminating the effects of varying atmospheric and insolation conditions.

2. REMOTE SENSING MODEL

Atmospheric gases and aerosols modify the incident solar radiation as well as the radiation reflected from the surface by attenuating it and by changing its spatial distribution. The result is a blurred image of the objects. Dark surfaces, such as vegetation or water in the visible spectral region, are brightened by path radiance. Bright surfaces, such as vegetation in the near infrared, are darkened by extinction of the reflected radiance. Furthermore the reflection from contrasty surfaces leads to a net transfer of radiance from bright surfaces into the line of sight of the sensor while the sensor itself points toward a dark target. The result of this background effect is a diminuishing of the effective ground resolution and is especially important for high resolution sensing systems.

The satellite signal in a given spectral band can be described by a remote sensing model which calculates the solar radiance reflected by a Lambertian surface and received by a sensor in space

- for a uniform surface or given a low ground resolution of the sensor as

$$L_{obs} = A \cdot (t_{dir} + t_{diff}) \cdot E_G/\pi + L_p \qquad (1)$$

- for a nonuniform surface and given a high ground resolution of the sensor as in the case of Landsat/TM or SPOT as

$$L_{obs} = A \cdot t_{dir} \cdot E_G/\pi + A_B \cdot t_{diff} \cdot E_G/\pi + L_p \qquad (2)$$

where L_{obs} = radiance observed, A = target reflectance, A_B = average background reflectance, E_G = global irradiance on the ground, t_{dir} = direct transmittance, t_{diff} = diffuse transmittance and Lp = path radiance.

3. ALGORITHM FOR ATMOSPHERIC CORRECTION

The atmospheric correction method was developed and tested using Landsat/TM data for forestry applications. Concept and implementation are however universal enough to be adopted to other sensors and applications.

The steps of the procedure are carried out with KALKUL (Kienzle, 1989), a programming system specially developed for pixelwise processing of digital images at the Abt. Luftbildmessung und Fernerkundung of Freiburg University. The code LOWTRAN 7 (Kneizys et al., 1988) is applied for all radiative transfer calculations. The calibration coefficients recommended by Hill (1989) are used for the calibration of the Landsat/TM data. The spectral responses of the TM bands are taken into consideration within the bandwidths and with values provided by the moments method (Palmer, 1984).

3.1 Selection of Radiometric Control Points

Atmospheric corrections of multispectral satellite data which are not merely based on climotological data or additional measurements must make certain assumptions on the reflection characteristics of observed surfaces. For this purpose it is important to select dark surfaces with stable optical characteristics over which the satellite signal carries primarily information on atmospheric scattering.

The most appropriate surfaces from the viewpoint of forestry remote sensing are vegetation and especially forest stands which fulfil the required re-

flection characteristics in the visible spectral region and exist in the image data in sufficient numbers as central objects of the evaluation. The suitability of vegetation stands for the calibration of multispectral data has already been tested and confirmed by other authors (Ahern et al., 1979; Fehlert, 1984; Kim, 1988).

A modified version of the method of Kaufman and Sendra (1988) is applied to identify the pixels representing the required dense, dark vegetation. First, areas with dense vegetation are identified by high values of a vegetation index (section 1). A low reflection in the near infrared (section 2) serves as a second criterion for the selection of dense, dark vegetation stands. The intersection of section 1 and 2 contains pixels with the required characteristics (Fig. 1).

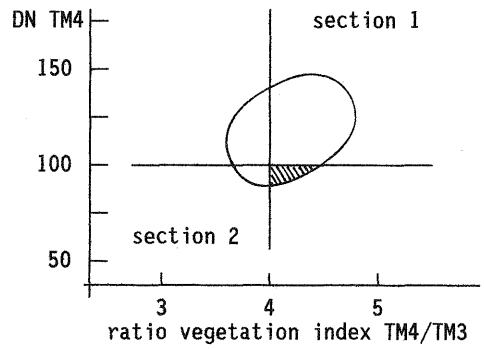

Fig. 1: Schematic Description of the Method for the Identification of Dense, Dark Vegetation from High Values of a Vegetation Index and a Low Reflection in the Near Infrared.

The size of the sections 1 and 2 is determined by an estimate of the vegetation area in the scene (Kattenborn, 1991). The scene is thus covered with a network of radiometric control points which, by means of radiative transfer calculations, serve to generate data on the actual local conditions of the atmosphere.

3.2 Modelling Atmospheric Conditions

3.2.1 Selection of an Aerosol Model and Computation of Atmospheric Data For an accurate correction of atmospheric effects in all spectral bands it is essential to select an appropriate aerosol model for the radiative transfer calculations. LOWTRAN aerosol models represent the optical characteristics of the aerosols and their wavelength dependency. Conversely the aerosol optical thickness calculated in two of the spectral bands of the image data supplies according to its wavelength dependence information on the required aerosol model according to

$$v = - \ln(\tau_{A1}/\tau_{A2})/(\ln(\lambda_1/\lambda_2) \qquad (3)$$

where v = wavelength exponent of aerosol extinction, τ_{A1}, τ_{A2} = aerosol optical thicknesses for wavelengths λ_1 and λ_2.

This relation can be used to infer the particle size distribution from the wavelength exponent with a precision sufficient for remote sensing applications (Kaufman and Fraser, 1983).

Using various aerosol models LOWTRAN calculates the mean aerosol optical thicknesses in bands TM1 and TM3 over the radiometric control points. Considering reflectance values measured for vegetation stands the calculation is based on a surface reflectance of 0.025 in TM1 and 0.030 in TM3 (Kattenborn, 1991). Eq. 3 calculates from the aerosol optical thicknesses the wavelength exponent of the extinction for each aerosol model tested. The wavelength exponents calculated in this way from the image data are now compared with the wavelength exponents of the aerosol models for the standard aerosol concentrations provided by LOWTRAN. The aerosol model with the closest correspondence is used for all further calculations.

This aerosol model and the assumed reflectance for dense, dark vegetation serve to determine the aerosol concentration over the individual radiometric control points in band TM1. It is used for the calculation of the values for transmittance, path radiance and global irradiance in all spectral bands under correction. If a digital terrain model is available, the altitude of the radiometric control points can be considered by a modification of the aerosol profile in the atmosphere boundary layer.

3.2.2 Smoothing and Interpolation of the Atmospheric Data For the atmospheric correction of a scene atmospheric parameters must be determined for each pixel. The atmospheric data calculated over the radiometric control points are therefore smoothed by cubic spline regression and values of the parameters are stored simultaneously for each pixel. This is an efficient way to smooth high frequency noise of the atmosphere parameters during the horizontal and vertical modelling of the required regional changes in atmospheric conditions. The result are radiometric data available for the application of the correction model at each pixel as shown in Fig. 2 with the example of the aerosol optical thickness in band TM1 of a Landsat/TM scene of an area near Freiburg taken in 1984. The digital terrain model on Fig. 2 shows that the aerosol optical thickness values from the image data are largely correspondent with the changes in the terrain.

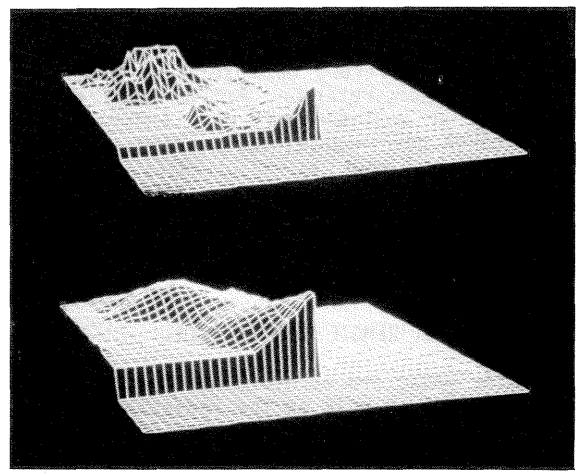

Fig. 2: Three-Dimensional Diagrams of the Terrain Model (Above) with Altitudes Ranging from 180 m to 700 m and the Aerosol Optical Thickness in Band TM1 Varying from 0.78 to 0.63 (Below) Derived from the Image Data of a Landsat/TM Scene of an Area Near Freiburg Taken in 1984.

3.2.3 Iteration of the Atmospheric Correction Model Owing to the lack of necessary information on background reflectance it is assumed that the pixel reflectance and the average background reflectance are identical. Inversion of Eq. 1 thus allows to derive pixelwise the surface reflectance for the scene under correction. The resultant reflectances are taken as a first estimate of the background reflectance.

The next step is to apply the inversion of Eq. 2 considering the background effects, and to re-apply the calculated reflectances to determine the background reflectances. The procedure is iterated until the differences in atmospherically corrected reflectances in subsequent calculations have fallen below a threshold defined according to the radiometric resolution of the sensor.

The average background reflectances are calculated with a 51 x 51 pixel matrix. With regard to the ground resolution of Landsat/TM the method thus follows measurements and calculations of background effects by various authors (Ueno et al., 1978; Tanre et al., 1981; Dana, 1982) in assuming a "radius" of 750 m around each pixel.

The assumption is that the background reflectance decreases toward the outside until pixel projections and scattering angles in the atmosphere become negligibly small so that the path lengths of the scattered photons (Bakan and Quenzel, 1976) become too long for a noticeable effect on the target signal.

The weighting of the reflectances from neighbouring pixels is therefore calculated in inverse proportion to the radius as

$$G_k = 1/(8 \cdot k^2 \cdot \sum_{i=1}^{n} 1/i) \qquad (4)$$

where G_k = weight of neighbouring pixel with actual radius k (in pixels), n = total radius.

4. RESULTS

An area near Freiburg, Germany of about 24 km * 15 km is used to illustrate results of the atmospheric correction method. The area encompasses parts of the Rhine Valley, the Kaiserstuhl mountain and the western slopes of the Black Forest with altitudes ranging from 180 m to 700 m. The Landsat/TM scenes were recorded on 23 July 1984 (path 195, row 27), 27 June 1986 (path 195, row 27) and 25 May 1989 (path 196, row 26).

4.1 Atmospherically Corrected Image

For a visual evaluation of the correction results Fig. 3 compares the atmospherically corrected data of band TM1 from the 1984 Landsat/TM scene with the original data.

Even at first glance the atmospherically corrected image appears sharper and richer in contrasts. This is due to an enhanced detail visibility which applies to all forms of land usage. Farmland shows a clearer structuring and parcelling than in the uncorrected image. The correction has also produced a sharper distinction between forest and non-forest areas. Within the forest parts of the infrastructure are discernible such as forest stand delineations through the road network.

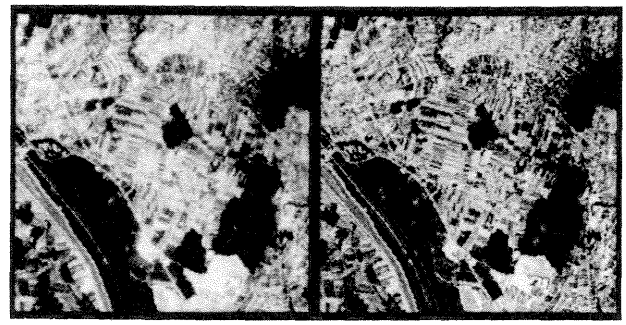

Fig. 3: Enlargement of a Section from the Original Band (Left) and the Atmospherically Corrected Band TM1 (Right) from a Landsat/TM Scene of an Area Near Freiburg Taken in 1984.

4.2 Profiles of Pixel Values

For a detailed evaluation of the effects of atmospheric correction pixel value profile were established for identical lines from the atmospherically corrected and the uncorrected band TM1 from the Landsat scene recorded in 1984. Comparability was ensured by selecting a line with an almost identical amplitude of corrected and uncorrected values (Fig. 4).

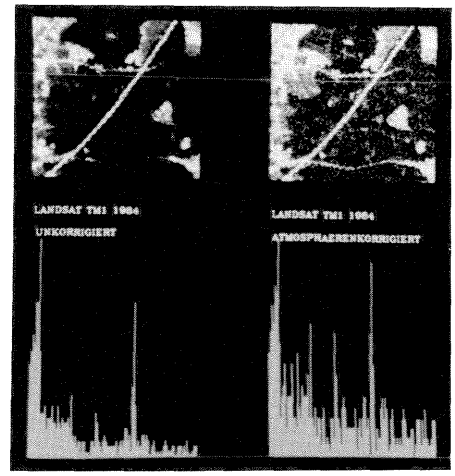

Fig. 4: Pixel Value Profiles of an Image Line in the Original (Left) and the Atmospherically Corrected Band TM1 (Right) from a Section of the Landsat/TM Scene of Freiburg Taken in 1984.

The comparison of the profiles confirms that atmospheric correction increases the dynamics of the data considerably, and therefore the contrast.

4.3 Standardized Photo Products

When original grey values are used neither standard transformations due to changes in observation conditions, nor scene specific transformations due to changes in the contents of the scenes allow a standard colouring of photo products from various scenes. It is therefore difficult for the interpreter to distinguish the actual changes from one scene to another from the artefacts of image enhancement.

With atmospherically corrected data, which are largely undistorted by changes in sensing conditions, it is however possible through standard transformation to produce photo products of each Landsat/TM scene with constant colouring.

The photos in Fig. 5 were generated from the atmospherically corrected 1984 and 1986 Landsat/TM scenes through a linear transformation of bands TM7, TM4 and TM3. The upper and lower limits of the reflectances to be transformed (see Table 1) were specially selected for forestry application closely following Ahern and Sirois (Ahern and Sirois, 1989).

band	TM1	TM2	TM3	TM4	TM5	TM7
min. refl.	-0.01	-0.01	-0.01	-0.01	-0.01	-0.01
max. refl.	0.12	0.15	0.17	0.53	0.35	0.21

Table 1: Linear Transformation Limits for the Generation of Standard Photo Products for Forestry Applications from Atmospherically Corrected Reflectances.

The photo products allow the forested areas to be clearly identified through their colouration and thus provide a good survey of the region's forest ratio. Within forests deciduous and coniferous stands differ from each other by their varying light and dark green colouring. This, in addition to the constancy in colouring (see Fig. 5 left and right), is another advantage of photo products standardized in this way which, by selection of the spectral bands and the transformation limits, can be further refined similar to thematic maps with classes distinguished by colours.

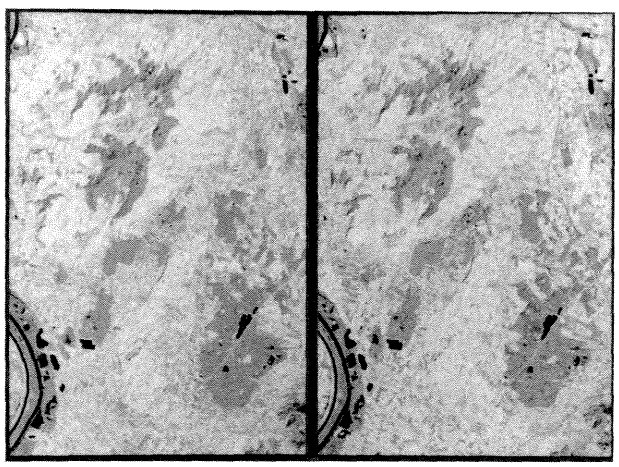

Fig. 5: Standard Photo Products Refined for Forestry Applications. The Images Were Generated by a Linear Transformation of Atmospherically Corrected Reflectances in Bands TM7, TM4 and TM3 from Landsat Scenes of Freiburg Recorded in 1984 (Left) and 1986 (Right).

5. VERIFICATION

5.1 Multitemporal Comparison

The time series of 1984, 1986 and 1989 which are shown in Table 2 consist of the average original grey values and atmospherically corrected reflectances in the bands of Landsat/TM scenes of the southern Upper Rhine Valley.

In contrast to the average grey values which vary considerably in the individual bands the averages of atmospherically corrected reflectances are largely correspondent. The average reflectance of the area appears to be relatively stable at the various recording dates, while the variations of atmospheric conditions and sun angles which are recognizable in the differences in the average grey values, were for the most part eliminated in the correction.

	TM1	TM2	TM3	TM4	TM5	TM7
scene	atm. corrected reflectances					
1984	0.066	0.109	0.120	0.518	0.292	0.189
1986	0.066	0.111	0.110	0.501	0.297	0.197
1989	0.067	0.112	0.122	0.476	0.308	0.218
	original grey values					
1984	88.4	38.0	37.3	94.6	79.0	31.9
1986	82.9	37.5	35.3	98.9	86.0	36.0
1989	79.6	36.5	36.8	92.4	70.3	38.7

Table 2: Average Original Grey Values and Atmospherically Corrected Reflectances of the Southern Upper Rhine Valley in the Bands of Landsat/TM Scenes from 1984, 1986 and 1989.

5.2 Background Effect Correction

Small water bodies are a good example to demonstrate the necessity and efficacy of background effect correction. This study uses the spectral signatures of a lake from the 1984 Landsat/TM scene of Freiburg which is closely surrounded by forest and 500 m in diameter. To avoid distortions from signal components from the lake bottom near the banks pixels toward the centre were selected for a spot check.

Exoatmospheric reflectances were calculated as well as path radiance corrected reflectances prior to background radiance correction and both path radiance and background radiance corrected reflectances as the final products of the correction procedure (Fig. 6).

The uncorrected and merely path radiance corrected signature of the lake are marked by a peak in band TM4, the spectral region of maximum reflection of vegetation. These values which are unusually high for the reflection from water bodies in the near and middle infrared are due to the background contribution from the surrounding vegetation. In this case only background effect correction produces a signature which is typical for water because the reflectance from clear water in the infrared spectral regions is zero. The difference between the background effect corrected signature and this level can be taken as an indication for the precision of the method of atmospheric correction owing to the fact that this particular lake is relatively clear.

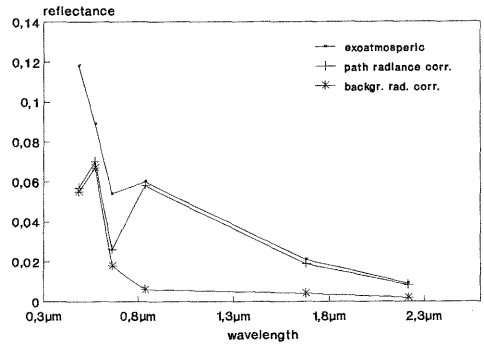

Fig. 6: Exoatmospheric, Path Radiance Corrected and Both Path Radiance and Background Radiance Corrected Signatures of a Lake from the 1984 Landsat/TM Scene of Freiburg.

5.3 Sensitivity to the Assumed Reflectance of the Radiometric Control Points

The reflectance assumed in the radiative transfer calculations for dense, dark vegetation has an immediate effect on the values calculated for path radiance, transmittance, global irradiance and the correction result itself which has been calculated on the basis of these data. It is therefore important to give an estimate of the imprecision of the correction result which is tied to the reflectance assumed for the radiometric control points.

Table 3 shows the atmospherically corrected reflectances for the mean grey values of the Landsat/TM scene from 1984 when the assumed reflectance of the radiometric control points in band TM1 changes by 0.01. In band TM1 a change in the assumed reflectance by 0.01 produces a change of the atmospherically corrected reflectance of the same size. In the other bands the change is considerably smaller.

refl. rad.c. points	atm. corrected reflectances					
	TM1	TM2	TM3	TM4	TM5	TM7
0.025	0.067	0.108	0.116	0.522	0.264	0.167
0.015	0.057	0.102	0.112	0.526	0.267	0.167

Table 3: Atmospherically Corrected Reflectances for the Mean Grey Values of the Landsat/TM Scene of Freiburg Taken in 1984 when the Reflectance of the Radiometric Control Points in Band TM1 Assumed in the Calculation of Atmospheric Data is Changed from 0.025 to 0.015.

6. CONCLUSION

Landsat/TM was used as an example for the development of an algorithm for atmospheric correction of multispectral satellite data. The method requires only one data set and can be applied to any ground resolution provided that the scene contains patches of dense, dark vegetation beyond pixel size.

Among vegetation types especially forest areas (Kattenborn, 1991) provide controllable surfaces which can be used to establish a network of radiometric control points for the calculation of the required atmospheric data. These data correspond with the actual local atmospheric conditions over a scene in contrast to algorithms which use visibility estimates or assume standard atmospheric conditions.

Information on the reqired aerosol model, e.g. the aerosol phase function, is also gathered from the image data. The method used for this purpose can be applied to all imaging systems which have at least two bands within the visible spectral region (Kaufman and Fraser, 1983). A possible imprecision of the single scattering albedo, e.g. the aerosol absorption, which cannot be determined from the image data might be balanced by the inclusion of the value for the single scattering albedo both in the calculation of the aerosol optical thickness over the radiometric control points and in the path radiance values employed in the correction model.

Almost completely based on image data atmospheric parameters are calculated with a minimum of generalising climatological data. Correspondingly the atmospheric correction model is designed for operational use independent of further input. However, although producing good results the correction model also illustrates the limits of ground reflectance calculation from multispectral satellite data, since each refining of the correction model requires additional input data which must be correspondingly precise. An equation for the exact description of the radiation field over a pixel could in this context serve as an extreme example. It would require precise information on the surface reflection characteristics before it could be solved to calculate these reflection characteristics. This lack of a priori information is compensated for by generally presupposing Lambertian surfaces. According to Lee and Kaufman (1986) this assumption is justified for nadir or almost nadir observations as in the case of Landsat/TM.

Possible anisotropy effects are less important in multitemporal interpretations and monitoring tasks using atmospherically corrected data provided the same sensing system with the same observation geometry is used. Furthermore Koepke (1986) has presented a possible solution through the description and calculation of anisotropy conversion factors for the surface types coniferous forest, pasture and arable land which could be used for anisotropy correction by subsequent processing.

As shown with the example of a water body, the iterative approximation for background effect correction based on a pixel "radius" of 750 m has turned out to be efficient.

Results of multitemporal comparisons of targets with stable reflection and a sensitivity analysis have shown that an absolute precision of 0.01 can be reached in atmosphere corrected reflectances (Kattenborn, 1991). A correction method which takes neither horizontal nor vertical changes in atmosphere conditions into account would certainly be less precise.

Albedo images generated with the correction model are much easier to comprehend in visual and digital interpretation because in contrast to the original data they represent intrinsic surface characteristics. The reached precision allows the production of standard photos which could be used as survey maps. It seems to suffice for such monitoring tasks as the study of changes in forest areas or land usage. These monitoring demands require new efforts in the visual and digital interpretation of the corrected images. Particularly the input of atmo-

sphere corrected, and thus largely standardized data into information systems is likely to improve the methods of interpretation. With the trend to a rationalization of the interpretation the correction of external effects becomes more and more important because reliable radiometric correction helps to reduce the number of problem solutions which a interpretation or expert system has to take into account.

7. REFERENCES

Ahern, F. J., Teillet, P. M. and Goodenough, D. G., 1979. Transformation of atmospheric and solar illumination conditions on the CCRS image analysis system. In: Proc. of the 5th Annual Symp. on Machine Processing of Remotely Sensed Data, West Lafayette, Indiana pp. 34-52.

Ahern, F. J. and Sirois, J., 1989. Reflectance enhancements for the Thematic Mapper: An efficient way to produce images of consistently high quality. Photogrammetric Engineering and Remote Sensing 58: 61-67.

Bakan, S. und Quenzel, H., 1976. Weglängenverteilungen gestreuter Photonen in aerosolhaltigen Atmosphären. Beiträge zur Physik der Atmosphäre 49: 272-284.

Dana, R. W., 1982. Background reflectance effects in Landsat data. Applied Optics 21: 4106-4111.

Fehlert, G.-P., 1984. Kalibrierung von MSS-Satellitenbilddaten zur Auswertung zeitlicher Reflexionsänderungen an Fichtenbeständen. DLR-Forschungsbericht, DFVLR-FB84-44.

Hildebrandt, G., Kadro, A., Kuntz, S. and Kim, C., 1987. Entwicklung eines Verfahrens zur Waldschadensinventur durch multispektrale Fernerkundung. Forschungsbericht KFK-PEF25.

Hill, J., 1989, Monitoring crops and natural vegetation using Landsat TM data. In: Ispra Courses: Remote Sensing for vegetation monitoring. 10. - 14. April 1989. Commission of the European Communities, Joint Research Centre Ispra, Italy.

Kattenborn, G., 1987. Das Reflexionsverhalten von gesunden und geschädigten Weißtannen unter dem Einfluß von Standort und Aufnahmebedingungen. Diplomarbeit, Universität Freiburg.

Kattenborn, G., 1991. Atmosphärenkorrektur von multispektralen Satellitendaten für forstliche Anwendungen. Dissertation, Universität Freiburg.

Kaufman, Y. J. and Fraser, R. S., 1983. Light extinction during summer air pollution. Journal Appl. Meteor. 22: 1694-1706.

Kaufman, Y. J. and Sendra, C., 1988. Algorithm for atmospheric corrections to visible and near IR satellite imagery. International Journal of Remote Sensing 9: 1357-1381.

Kienzle, R.-P., 1989. KALKUL - Universal programming system for pixelwise processing of digital images. Users Manual, Abt. Luftbildmessung und Fernerkundung, Universität Freiburg (unpublished).

Kim, H. H., 1988. Atmospheric effect removal from space imagery. In: Proc. of the 4th Int. Colloquium on Spectral Signatures of Objects in Remote Sensing, Aussois, France, 18.-22. Jan. 1988, ESA SP-287. pp. 193-196.

Kneizys, F. X., Shettle, E. P., Abreu, L. W., Anderson, G. P., Chetwynd, J. H., Gallery, W. O., Selby, J. E. A. and Clough, S. A., 1988. Users guide to LOWTRAN 7. Air Force Geophysics Laboratory Hanscomb AFB, Massachusetts. AFGL-TR-88-0177.

Koepke, P., 1986. Clear land anisotropy conversion factors: A comparison of theoretical and experimental results. In: Proc. ISLSCP Conference, Rome, Italy. ESA SP-248. pp. 271-276.

Lee, T. and Kaufman, Y. J., 1986. Non-lambertian effects on remote sensing of surface reflectance and vegetation index. IEEE Transactions Geoscience and Remote Sensing GE-24: 699-708.

Palmer, J. M., 1984. Effective bandwidth for Landsat 4 and Landsat-D Multispectral Scanner and Thematic Mapper subsystems. IEEE Transactions Geoscience and Remote Sensing GE-22: 336-338.

Schardt, M., 1990. Verwendbarkeit von Thematic Mapper-Daten zur Klassifizierung von Baumarten und natürlichen Altersklassen. Dissertation, Universität Freiburg.

Tanre, D., Herman, M. and Deschamps, P. Y., 1981. Influence of the background contribution upon space measurements of ground reflectance. Applied Optics 20: 3676-3684.

Ueno, S., Haba, Y., Kawata, Y., Kusaka, T. and Terashita, Y., 1978. The atmospheric blurring effect on remotely sensed Earth imagery. In: Fymat, A. L. and Zuev, V. E. (Eds.): Remote Sensing of the Atmosphere: Inversion Methods and Applications. New York: Elsevier, p. 305.